Characterization of As-polluted soils by laboratory X-ray-based techniques coupled with sequential extractions and electron microscopy: the case of Crocette gold mine in the Monte Rosa mining district (Italy)

Arsenic speciation and mobility in polluted soils revealed by a multianalytical approach using X-ray based techniques, sequential extractions and electron microscopy

Ignazio Allegretta[a,*], Carlo Porfido[a], Maria Martin[b], Elisabetta Barberis[b], Roberto Terzano[a], Matteo Spagnuolo[a]

[a] Dipartimento di Scienze del Suolo, della Pianta e degli Alimenti, Università degli Studi di Bari "Aldo Moro", Via G. Amendola 165/A, 70126 Bari (Italy)

[b] Dipartimento di Scienze Agrarie, Forestali e Alimentari, Università degli Studi di Torino, Largo Paolo Braccini 2, 10095 Grugliasco – Torino (Italy)

*ignazio.allegretta@uniba.it Tel: +39 080 5443574; Fax: +39 080 5442850

Abstract

In the present study, a multianalytical approach was used to characterize arsenic (As) polluted soils. Arsenic speciation and speciation were studied by combining X-ray based techniques (WDXRF, μXRF and XRPD) with field emission scanning electron microscopy equipped with microanalysis (FE-SEM-EDX) and sequential extraction procedure (SEP) coupled to total reflection X-ray fluorescence (TXRF) analysis. This approach was applied to three contaminated soils and one mine tailing collected near the gold extraction plant at the Crocette gold mine (Macugnaga, VB), in the Monte Rosa mining district (Piedmont, Italy). The As concentration in the samples was measured with WDXRF and ranged from 145 to 40200 mg/kg. XRPD showed the presence of jarosite and the absence of any As-bare mineral suggesting a high weathering grade and strong oxidative conditions. However, small domains of scorodite were identified by combining μXRF with FE-SEM-EDX. SEP results revealed that As was mainly associated to amorphous Fe-oxides/hydroxides (50/80%)

and the combination of XRPD and FE-SEM-EDX suggested that this phase can be shwertmannite. On the basis of the soils and tail characteristics, As is scarcely mobile, even if a consistent As fraction (1-3 g As per kg of soil) is still potentially mobilizable. Such multianalytical approach could be used as a standard strategy for risk assessment evaluation of As contaminated soils, requiring only commercial laboratory equipment.

Keywords

Arsenic speciation, soil, gold mine, X-ray analysis, microanalysis

1. Introduction

Arsenic (As) is a natural constituent of the earth crust and it can occur in concentration of 0.1-500 mg/kg according to the rock or soil genesis (Mandal and Suzuki, 2002). However, in some cases it can reach very high concentration due to industrial or mining activities (Vaughan, 2006). The chronic exposure by ingestion of As is dangerous for human and animal health (Eisler, 2004; Hopenhayn, 2006). For this reason particular attention has been paid on the assessment of its bioavailability (Allegretta et al., 2017; Kim et et., 2014; Niazi et al., 2011; Porfido et al., 2016) and restrictions have been imposed for the total concentration of As in water and soils (Decree of the Italian Ministry Council, 2006; WHO, 2011). However, the As total concentration does not reflect the real potential risk of the element since not all the As forms are mobile and bioavailable. Depending on pH and redox potential, the two most common forms of As in soils are the dissociation products of H_3AsO_4 and H_3AsO_3 (Mandal and Suzuki, 2002; Morin and Calas, 2006; Smedley and Kinninburgh, 2002). These arsenate and arsenite species, as secondary As-bare minerals (i.e. scorodite, arsenolite and claudetite), are usually the oxidation products of primary minerals such as arsenopyrite, orpiment and realgar (Drahota and Filippi, 2009). Arsenic mobility depends strictly on pH and redox conditions (Masscheleyn et al., 1991; Smedley and Kinninburgh, 2002; Zobrist et al., 2000), but other parameters such as the chemical and mineralogical

composition of the soil (Lenoble et al., 2002; Violante and Pigna 2002) and the microbial activity (Fendorf et al., 2008; Lloyd and Oremland, 2006) can influence it as well. Due to the complexity and heterogeneity of the soil system, a correct characterization and mobility assessment of As can be done only using multianalytical approaches (Haffert and Craw, 2008; Kocourkovà-Viškovà et al., 2015; Lu and Zang, 2005; Marabottini et al., 2013). Among all the available analytical techniques, X-ray based spectroscopies proved to be useful tools for the investigation of polluted soils. In particular, X-ray fluorescence spectroscopy (XRF) is a fast, non destructive and reliable technique for the determination of As concentration (Parson et al., 2013; Radu and Diamond, 2009). X-ray diffraction (XRD) is widely used to study the mineralogical composition of soils and, combined with X-ray absorption spectroscopy (XAS) or X-ray photoelectron spectroscopy (XPS), provides information about As-minerals or its oxidation forms (Arčon et al., 2005; Drahota et al., 2009; Javed et al., 2014; Kim et al., 2013; Lumsdon et al., 2001; Savage et al., 2000; Strawn et al., 2002). Finally, μXRF and scanning electron microscopy coupled with energy dispersive x-ray fluorescence spectroscopy (SEM-EDX) give information about the elements distribution in the sample and its microstructure (Haffert and Craw, 2008; Strawn et al., 2002).

In most of these studies, synchrotron X-ray based techniques have been adopted, thus making them not easily reproducible, especially for those scientists not having access to these facilities. Although these techniques cannot directly assess As mobility, they are often used to predict it. Moreover, their integration with sequential extraction procedures (SEP) can give a deeper understanding of the As mobility in polluted soils (Drahota et al., 2009; Javed et al., 2014; Kim et al., 2013; Lu and Zang, 2005).

In the present work we used a multianalytical approach combining laboratory X-ray based techniques (WDXRF, μXRF and XRPD), field emission scanning electron microscopy coupled with microanalysis (FE-SEM-EDX) and a sequential extraction procedure (Wenzel et al., 2001) to characterise As-polluted soils and assess As speciation. In addition, a new hyperspectral XRF data analysis method was used for the first time on soil samples.

As a case study, three soils and a mine tailing, sampled from the abandoned gold mining site of Crocette (Monte Rosa, Piedmont, Italy), were investigated. Such multianalytical approach allowed to understand the actual concentrations and the dominant chemical forms of As, as well as the mechanisms controlling its mobility and bioavailability. This type of information is of paramount relevance in environmental risk studies and cannot be gathered by simple standard analytical methodologies. The multianalytical approach presented in this study is proposed for all those studies aiming at understanding the evolution and the risks associated to As in abandoned mining sites which can still endanger the surrounding environment.

2. Materials and methods

2.1 Sampling and preliminary analyses

The samples (three soil and one mine tailing samples) were collected near the remains of the plant for gold extraction located at Crocette (1400 m s.l.m.), along the Quarazza creek, flowing in a small lateral valley on the right side of the Anzasca valley (Macugnaga, Piedmont, Italy) (Fig. 1). The plant, established in 1936, was definitively closed and dismissed in 1953. The plant, as well as some dumped mine tailings and flotation sediments, are located on a steep slope on the left side of the creek, mostly occupied by regosols and leptosols developing on metamorphic and igneous rocks of the Western Italian Alps (Costantini and Dazzi, 2013). Forest trees and herbaceous vegetation are covering almost completely the site. No data about As pollution are available in the literature about this specific site.

In order to collect the As-bearing samples, the element concentration was estimated *in situ* using a NITON XL3t 900 portable ED-XRF spectrometer (Thermo Scientific) equipped with a Ag target (40 kV, 50 μA). Three different soils (S1, S2 and S3) and one mine tailing (S4) were chosen for their different As content and sampled. The S1 sample was collected as a control sample on the

right side of the creek, much less affected by the activity of the plant than the soils on the left side. The soil samples S2 and S3, as well as the mine tailings, were collected around the plant within 50 m from it. After removing the organic undecomposed litter, the first 15-20 cm of soil (roughly corresponding to the soil A horizon) were collected. The samples were stored in plastic containers and transported to the laboratory where they were air dried. After quartering, textural, chemical and mineralogical analyses were carried out.

Soil texture was analysed using the pipette method (Indorante et al., 1990), pH was measured in double-distilled water and total organic carbon (TOC) was estimated using the Walkley-Black method (Sparks, 1996).

Major elements (Si, Al, Na, Mg, Ca, K, Ti, Mn, Fe, S and P) and As concentration were determined with WDXRF using a Supermini200 (Rigaku Corporation, Tokyo, Japan) spectrometer equipped with a Pd X-ray tube (50 kv, 4 mA) operating under vacuum (< 12 Pa). The instrument was calibrated using geological standards provided by SARM (Service d'Analyses des Roches et des Minéraux, CRPG-CNRS, Vandoeuvre-les-Nancy, France).

Mineralogical analysis was performed via XRPD using a Miniflex II (Rigaku Corporation, Tokyo, Japan) X-ray diffractometer equipped with a Cu tube (Cu Kα, 30 kV, 15mA). Data were acquired between 3 and 70 ° 2θ with a step width of 0.02° 2θ and a counting time of 3 s per step. The incident beam passed through a 0.3 mm Soller slit, 1.25° divergent slit, a 10 mm mask and emerged after a 1.25° antiscattered slit.

2.2 Sequential extraction procedure (SEP)

In order to assess the potential mobility of As in the studied soils, a five-step sequential extraction procedure (SEP), proposed by Wenzel et al. (2001), was applied. This SEP consists of the following steps:

1. *non-specifically adsorbed As* extracted with $(NH_4)_2SO_4$ 0.5 M for 4 h at 20 °C;
2. *specifically-sorbed As on minerals* extracted with $NH_4H_2PO_4$ 0.5 M for 16 h at 20 °C;

3. *As adsorbed on amorphous and scarcely ordered Fe and Al oxides and hydroxides* extracted with NH_4-oxalate 0.2 M for 4 h at 20 °C;
4. *As adsorbed on well-crystallized Fe and Al oxides and hydroxides* extracted with NH_4-oxalate 0.2 M and ascorbic acid 0.1 M for 30 min at 96 °C;
5. *residue* treated using microwave digestion with HNO_3 and H_2O_2.

After each extraction step the suspension was centrifuged for 15 min at 1700 × g and the solution was filtered through 0.45 μm cellulose acetate filters. The As concentration in the extracted solution was quantified via total reflection X-ray spectroscopy (TXRF) using a S2 Picofox spectrometer (Bruker Nano GmbH, Berlin, Germany) equipped with a Mo target (50 kV, 600 μA), a multilayer monochromator and a XFlash® silicon drift detector (energy resolution was less than 150 eV at 5 kcps at Mn Kα). In order to quantify As, 10 μl of Ga (100 mg/l) were added to 1 ml of filtered solution as internal standard. After vortexing, 10 μl of solution were pipetted onto a quartz carrier and left drying on a hot plate at 50 °C in a laminar flow hood. The analysis were done in triplicate and each sample was measured for 1000 s.

2.3 μXRF and FE-SEM-EDS analyses

In order to study the element distribution, μXRF analyses were carried out on petrographical thin sections of the sampled soils. For this purpose, a M4 Tornado spectrometer (Bruker Nano GmbH, Germany, Berlin) was used. The analysis were conducted with a Rh target (50 kV, 600 μA) and polycapillary optics having a spot size of 25 μm. The secondary x-ray fluorescence was collected by two XFlash® silicon drift detectors (FWHM < 140 eV at the Mn Kα) with an active area of 30 mm^2 placed at 45° to the X-ray source. The analysis were carried out under vacuum (20 mbar), using a sampling step of 20 μm for 10 ms. X-ray fluorescence hyperspectral data were processed using PyMca 5.1.3 (Sole et al., 2007) and Datamunchen (Alfeld and Janssens, 2015) softwares. A FE-SEM Zeiss Σigma 300 VP (Zeiss Oberkochen, Germany) working at 15 kV and equipped with an energy dispersive spectrometer (EDS) C-Max^N SDD with an active area of 20 mm^2 (Oxford

Instruments, Oxford, United Kingdom) was used to study the microscopic and submicrometric structure of the soils as well as the element association at this scale.

3. Results and discussion

3.1 Physicochemical and mineralogical characterization of the soils

Physical and chemical properties of the soils and mine tailing samples were determined and the results are reported in Table 1. All the samples are acid soils with a pH ranging from 3.6 to 4.3. They have a sandy loam texture with a sand fraction ranging between 56.0 and 65.7 %, a silt component between 24.9 and 33.3 % and a clay fraction of 9.4-15.0 %. They differ for the organic matter (OM) content which is higher in S1 (10.9 %) than in the other samples, in particular if compared with S4, where OM is only 2.5 %.

The chemical characterization of the soils and the tail from Crocette gold mine, performed with WDXRF, is reported in Table 2. Soils and tail show quite the same concentration of major elements (expressed as oxides) except for Fe_2O_3 and SO_3, much higher in S4 and S3. The As concentration in the three soils is different and increases from S1 (145 mg/kg) to S3 (13300 mg/kg), while in the mine tail (S4) it is 40200 mg/kg. All these values strongly exceed the Italian legislation limit for As in soils which is 20 mg/kg (Decree of the Italian Ministry Council, 2006). The As concentration is related to the sampling area. In fact, the mine tailing, which has the highest As concentration, was collected close to the abandoned factory (Fig. 1). The As concentration is lower in S2 and S3, which were collected 33 and 45 m from the abandoned mine factory. Finally, S1, which was collected on the other side of the creek, 130 m far from the factory, shows an As concentration three orders of magnitude lower than S2 and S3. Both Fe_2O_3 and SO_3 increase from S1 to S4 with As concentration (Table 2).

The mineralogy of the samples is mainly characterized by soil silicates and aluminosilicates: quartz, microcline, albite, illite and kaolinite (Fig. 2).

Smectite is clearly visible in S2 and weakly present in S1 while a weak hump of the 100% diffraction peak of sepiolite is observed in S2. Moreover, in sample S4, weak reflections at d = 3.11, 3.08, 5.09, 5.74 and 5.94 Å can be attributed to Jarosite ($KFe_3(SO_4)_2(OH)_6$) (Warshaw, 1956), which usually forms from the oxidation of pyrite (or arsenopyrite) in presence of K and in very acid environments (Fanning et al. 2002;Kim et al., 2014; Savage et al., 2000). No primary As-bearing minerals (e.g. arsenopyrite, orpiment, realgar) or secondary phases (e.g. Fe arsenates and sulphoarsenates) were detected in the samples by XRPD. Two small peaks at d = 2.54 and 1.51 Å could be attributed to scarcely ordered Fe-oxides/hydroxides, and in particular they could belong to ferrhydrite ($Fe_5HO_8 \cdot 4H_2O$) or shwertmannite ($Fe_8O_8(OH)_6SO_4$). Although the mineral identification cannot be done univocally, due to the absence of the weakest reflections and the low intensity of the main peaks, schwertmannite seems to be the most probable Fe-mineral since it forms at pH = 3 - 4 in presence of high concentration of sulphates. Despite the weakness of the diffraction peaks of these Fe-oxides/hydroxides, they are present in the soils and tail in very high amounts (see next paragraph), most probably as not well crystallized forms. The presence of short-range ordered Fe-oxides/hydroxides phases could be due to the high sulphate concentration which hinders their crystallization from amorphous Fe-oxides/hydroxides (Langmuir et al., 1999).
The absence of both arsenopyrite and pyrite, the occurrence of poorly crystalline to amorphous Fe-oxides/hydroxides and small amount of jarosite testify the high degree of weathering of these samples, which surely occurred under oxidizing conditions.

3.2 As distribution in the soils

µXRF chemical maps (Fig. 3) show that the As signal increases moving from S1 to S4 and the same is observed for Fe and S. All these three elements are generally found in the same sample areas, excluding some spots in which there is only the co-presence of As and Fe. It can be noticed that As and Fe are always present in the same regions and form aggregates around silicates or aluminosilicates (Si map). The correlations between Fe and As are clearly visible in Fig. 4a. The

scatterplot (obtained by plotting the K-lines signals of As and Fe) shows that three different As/Fe ratios can be identified. Excluding the blue group, (Fig. 4a) which represents Fe-rich domains, the largest part of the points belongs to the As/Fe ratio represented by the red area (Fig. 4b). Moving from low As-concentration to high As-concentration soils, the areas which show such As/Fe ratios increase at the expenses of Fe-rich components (blue group). Only few sampled points show a higher As/Fe ratio (marked with the green lines). However, the domains belonging to this ratio are very small (< 100 μm) and were detected only in S3 and S4 (Fig. 4c). At a higher resolution, FEG-SEM-EDX analyses (Fig. 5) show that the sample areas which belong to the As/Fe ratio in the "red regions" of Fig. 4 are mainly soil aggregates whose composition is variable. Iron is the major element followed by As. However, in some cases S is also detected. This variable composition can explain the point dispersion of the red group (Fig. 4a). As an example, Fig. 5a reveals that darker grey regions (characterized by Fe and As) are covered by brighter particles rich in Fe and S and where the As signal is sensibly reduced (Fig. 5b and 5d). However, these objects do not show a fixed chemical composition and therefore their nature cannot be clearly defined. XRPD reveals no As-Fe mineral but, looking at SEP data (Table 3) this variable composition could be due to the adsorption of As on amorphous and/or scarcely ordered Fe-oxides/hydroxides, which represent 50-80 % of the total As (see next paragraph). On the contrary, FEG-SEM-EDX analysis on the "green areas" of Fig. 4 (Fig. 6a) evidenced the presence of very few bright minerals of 20-50 μm whose composition is fixed and characterized by the presence of As and Fe. Semiquantitative EDX (Fig. 6b) analysis of this mineral suggest that it is probably scorodite and, due to its low concentration, it is not detected via XRPD. Scorodite could form at pH < 3 (Drahota et al., 2009; Langmuir et al., 2006) and the kinetic of formation increases with the decrease of pH (Patnurk et al., 2008). In the case of the soils and mine tailing form Crocette, the pH ranges between 3.6 and 4.3 (Table 1) which is higher than the stability range of scorodite and, according to Patnurk et al. (2008), in this pH range the kinetics for scorodite formation is very slow. This justifies its scarse presence in soils and mine tailing samples. On the contrary, the pH of the samples is more suitable for the formation of

Fe oxides/hydroxides (which require a pH > 3 and oxidative conditions) after the weathering of pyrite and arsenopyrite, hindering the crystallization of jarosite which, in fact, is weakly present only in S4 (it requires a pH < 3.5) (Fanning et al. 2002).

3.3 Prediction of As mobility

Arsenic mobility is closely connected to As speciation and to the soil phases to which it is bound. Important information on the mobility of As can be derived from SEP data (Table 3). Each step of the SEP can be linked to a particular soil fraction to which As is bound (or adsorbed) and the strength of As interactions with the soil phases increases at higher extraction steps.

Excluding S1, more than 90% of the total As in S2, S3 and S4 samples is extracted in the first three steps. The mine tailing (S4) is the sample which has the largest exchangeable As fraction (step 1, 11.7 % of total As), corresponding to soluble As forms. This means that 4.7 g of As per kg of tailing are potentially highly mobile. This fraction is less relevant in soils S2 and S3, where it accounts only to 0.6 and 0.2 %, respectively, which corresponds to 27 mg of As per kg of soil (in both samples), suggesting a sudden, strong decrease in soil As mobility when moving away from the tailing dump.

The As specifically adsorbed to soil particles (step 2) ranges from 6.7 to 25.2 % of the total As, which means that 1-3 g of As per kg of soil could be mobilized by phosphates. However, even by assuming that the total amount of phosphate-extractable As in the sample is mobile (which is far from reality), still only a little part of As could be mobilized.

As mentioned in the previous section, the As adsorbed on amorphous Fe-oxides/hydroxides is the most represented fraction and is likely to be scarcely mobile (in particular in presence of schwertmannite), especially in such oxidizing environment. In fact, a number of As immobilization strategies exploit amorphous Fe-oxides/hydroxides for reducing the risks associated with As pollution (Drahota et al., 2009; Nazari et al., 2016). Moreover, amorphous Fe-oxides/hydroxides are stable in a wide pH range, which make them more appropriate for As stabilization than other

minerals, like scorodite (Burton et al., 2009; Nazari et al., 2016). The mobility of As bound to Fe-oxides/hydroxides depends on pH and redox potential and could be increased by either a desorption of As from these phases or the hydrolysis of Fe-oxides/hydroxides. In the first case, the desorption of As from Fe-oxides/hydroxides is observed under oxidizing condition at pH > 8 (Lumsdone et al. 2001). Only when the concentration of Fe-hydroxides is lower than 1 %, the As desorption can occur at lower pH (about 6) (Lumsdone et al. 2001). All the studied samples have a low pH and in oxidizing conditions the As extracted in this step could be assumed to be non-mobile. In the studied field conditions, the most stable As form is $H_2AsO_4^-$ (Smedley and Kinniburgh, 2002). However, if the environmental conditions would change from oxidizing to reducing, the reductive dissolution of the iron (hydr)oxides could induce As release in solution (Smedley and Kinniburgh, 2002), and the concurrent reduction of arsenate to arsenite, that is poorly retained by clay minerals and Al oxides (Martin et al., 2014).

The hydrolysis of Fe-oxides/hydroxides could occur at pH < 2 (Bigham et al., 2002; Cornell et al., 1989; Fanning et al., 2002) but this condition is hardly reached in soils.

Another factor which affect the stability of Fe oxides/hydroxides is the reducing soil organic matter. Soluble organic matter can cause the hydrolysis of Fe-oxides/hydroxides due to the complexation of Fe^{3+} (Lindsay, 1991). Moreover, organic matter can compete with As for the adsorption on Fe oxides/hydroxides (Bauer and Blodau, 2006). This parameter could influence mobility of As in particular the in sample S1, where the TOC exceeds 10 %.

According to the literature (Kim et al., 2014; Niazi et al., 2011), the As extracted during the third step should be considered bioavailable, since amorphous Fe-oxides/hydroxides are considered non-stable phases. However, the potential bioavailability of this As fraction is not a consequence of its solubility, rather, it regards physiological strategies adopted by certain living organisms to mobilize iron from soil. This is observed for example with plants coping with iron deficiency that excrete protons and low molecules weight organic compounds to promote iron availability by solubilizing

in particular Fe-amorphous phases, thus increasing, among the others, As availability (Mimmo et al., 2014; Terzano et al., 2015).

The As extracted in steps 4 and 5 is important only in sample S1 where it represents the 27.9 and 9.4 % of the total As, respectively. However, the As associated to these two steps can be considered very stable because sorbed to crystalline phases (e.g. well-crystallized Fe-oxides/hydroxides, step 4) or included it in their lattice structure (e.g. sulphides, step 5).

4. Conclusions

In this study, a combination of different X-ray based analytical techniques (WDXRF, EDXRF, TXRF, XRD, μXRF), FE-SEM-EDX and a 5-step SEP was used to study As-polluted soils and tailings. In particular, samples from the abandoned gold mining site of Crocette (Italy) were investigated as a case study.

The combined approach allowed to get detailed information about As speciation and mobility in this site, otherwise not obtainable with conventional analytical methods.

Specifically, a strong weathering of the As-bearing minerals in the topsoil under oxidising and acidic conditions was observed, as evidenced by the absence of pyrite and arsenopyrite together with the occurrence of amorphous Fe-oxides/hydroxides and small amount of jarosite (in the mine tailing). .

No As-bare minerals were detected by XRPD. However, the combination of μXRF hyperspectral data analysis and FE-SEM-EDX allowed to identify small domains of Scorodite. In addition, by combining X-ray and microanalytical data with SEP additional information about As speciation and interaction with soil components was obtained. Arsenic was found mainly associated with poorly ordered Fe-oxides/hydroxides, which are known to limit the risk of As leaching and metalloid bioavailability (as evidenced by the growth of a plant coverage on the site despite of the very high As concentrations). However, an important amount of As was still potentially mobilizable

(1-3 g of As per Kg of soil) and should therefore be considered in environmental risk analyses and to foresee appropriate remediation actions.

A similar approach, based only on laboratory equipments, could be used systematically to study metal and metalloid pollutants in highly contaminated soils and sediments.

Acknowledgments

The present work is part of a project founded by Ministero dell'Istruzione, dell'Università e della Ricerca - Programmi di Ricerca Scientifica di Rilevante Interesse Nazionale Anno 2010-2011 – "Salubrità degli agroecosistemi: processi chimici, biochimici e biologici che regolano la mobilità dell'As nei comparti suolo-acqua-pianta".

All the analysis were performed at the *"Micro X-ray Lab"* of the University of Bari (Italy) supported by Regione Puglia (Programma Operativo Regione Puglia - FERS 2000-2006 - Risorse Liberate - Obiettivo Convergenza).

Dr. S. Stanchi is gratefully acknowledged for the pedologic advice.

Bibliography

Alfeld, M., Janssens, K., 2015. Strategies for processing mega-pixel X-ray fluorescence hyperspectral data: a case study on a version of Caravaggio's painting Supper at Emmaus. J. Anal. Atom. Spectrom. 30, 777-789. DOI: 10.1039/c4ja00387j

Allegretta, I., Porfido, C., Panzarino, O., Fontanella, M.C., Beone, G.M., Spagnuolo, M., Terzano, R., 2017. Determination of As concentration in earthworm coelomic fluid extracts by total-reflection X-ray fluorescence spectrometry. Spectrochim. Acta B. 130, 21-25. DOI: 10.1016/j.sab.2017.02.003

Arčon, I., van Elteren, J.T., Glass, H.J., Kodre, A., Šlejkovec, Z., 2005. EXAFS and XANES study of arsenic in contaminated soil. X-ray Spectrom. 34, 435-438. DOI: 10.1002/xrs.857

Bauer, M., Blodau, C., 2006. Mobilization of arsenic by dissolved organic matter from iron oxides, soils and sediments. Sci. Total Environ. 354, 179-190. DOI: 10.1016/j.scitotenv.2005.01.027

Bigham, J.M., Fitzpatrick, R.W., Schulze, D.G., 2002. Iron oxides, in: Dixon, J.B., Shulze, D.G. (Eds.), Soil Mineralogy in Environmental Application. Soil Science Society of America Inc., Madison, pp. 323-366.

Burton, E.D., Bush, R.T. Johnston, S.G., Walting, K.M., Hocking, R.K., Sullivan, L.A., Parker, G.K., 2009. Sorption of arsenic (V) and arsenic (III) to schwermannite. Environ. Sci. Technol. 43, 9202-9207. DOI: 10.1021/es902461x

Cornell, R.M., Giovanoli, R, Schneider, W., 1989. Review of the hydrolysis of iron(III) and the crystallization of amorphous iron(III) hydroxide hydrate. J. Chem. Tech. Biotechnol. 46, 115-134. DOI: 10.1002/jctb.280460204

Costantini, E., Dazzi, C., 2013. The Soils of Italy. Springer, Dordrecht, Heidelberg, New York, London.

Decree of the Italian Ministry Council, 2006. Norme in Materia Ambientale, Gazzetta Ufficiale, 88, 13–424

Drahota, P., Filippi, M., 2009. Secondary arsenic minerals in the environment: A review. Environ. Int. 35, 1243-1255. DOI: 10.1016/j.envint.2009.07.004

Drahota, P., Rohovec, J., Filippi, M., Mihaljevič, M., Pychlovský, P., Červený, V., Pertold, Z., 2009. Mineralogical and geochemical controls of arsenic speciation and mobility under different redox conditions in soil, sediment and water at the Mokrsko-West gold deposit, Czech Republic. Sci. Total Environ. 407, 3372-3384. DOI: 10.1016/j.scitotenv.2009.01.009

Eisler, R., 2004. Arsenic hazards to humans, plants and animals from gold mining. Rev. Environ. Contam. Toxicol.180, 133-165. DOI: 10.1007/0-387-21729-0_3

Fanning, D.S., Rabenhorst, M.C., Burch, S.N., Islam, K.R., Tangren, S.A., 2002. Sulfides and Sulfates, in: Dixon, J.B., Shulze, D.G. (Eds.), Soil Mineralogy in Environmental Application. Soil Science Society of America Inc., Madison, pp. 229-260.

Fendorf, S., Herbel, M.J., Tufano, K.J., Kocar, B.D., 2008. Biogeochemical processes controlling the cycling of arsenic in soils and sediments, in: Violante, A., Huang, P.M., Gadd, G.M., (Eds.), Biophysico-Chemical Processes of Heavy Metals and Metalloids in Soil Environments. John Wiley & Sons Inc. Hoboken, pp. 313-338.

Haffert, L., Craw, D., 2008. Mineralogical controls on environmental mobility of arsenic from historic mine processing residues, New Zealand. Appl. Geochem. 23, 1467-1483. DOI: 10.1016/j.apgeochem.2007.12.030

Hopenhayn, C., 2006. Arsenic in drinking water: impact on human health. Elements 2(2), 103-107. DOI: 10.2113/gselements.2.2.103

Indorante, S.J., Hammer, R.D. Koenig, P.G., Follmer, L.R. 1990. Particle-size analysis by a modified pipetted procedure. Soil Sci. Soc. Am. J. 54, 560-563. DOI: 10.2136/sssaj1990.03615995005400020047x

Javed, M.B. Kachanoski, G., Siddique, T., 2014. Arsenic fractionation and mineralogical characterization of sediments in the Cold Lake area of Alberta, Canada. Sci. Tot. Environ. 500-501, 181-190. DOI:10.1016/j.scitotenv.2014.08.083

Kim, E.J., Yoo, J.C., Baek, K., 2014. Arsenic speciation and biaccessibility in arsenic-contaminated soils: sequential extraction and mineralogical investication. Environ. Pollut. 186, 29-35. DOI: 10.1016/j.envpol.2013.11.032

Kocourková-Višková, E., Loun, J., Sracek, O., Houzar, S., Filip, J., 2015, Secondary arsenic minerals and arsenic mobility in a historical waste rock pile at Kaňk near Kuntá Hora, Czech Republic. Miner. Petrol. 109(1), 17-33. DOI: 10.1007/s00710-014-0356-0

Langmuir, D., Mahone, J., MacDonald, A., Rowson, J., 1999. Predicting arsenic concentrations in the porewaters of buried uranium mill tailing. Geochim. Cosmochim. Acta 63 (19/20), 3379-3394. DOI: 10.1016/S0016-7037(99)00259-8

Langmuir, D., Mahoney, J., Rowson, J., 2006. Solubility products of amorphous ferric arsenate and crystalline scorodite ($FeAsO_4 \cdot 2H_2O$) and their application to arsenic behavior in buried mine tailings. Geochim. Cosmochim. Acta 70, 2942-2956. DOI:10.1016/j.gca.2006.03.006

Lenoble, V., Bouras, O., Beluchat, V., Serpaud, B., Bollinger, J.C., 2002. Arsenic adsorption onto pillared clays and iron oxides. J. Colloid. Interf. Sci. 255, 52-58. DOI:10.1006/jcis.2002.8646

Lindsay, W.L., 1991. Iron oxide solubilisation by organic matter and its effect on iron availability. Plant Soil 130, 27-34. DOI:10.1007/BF00011852

Lloyd, J.R., Oremland, R.S., 2006. Microbial transformations of arsenic in the environment: from soda lakes to aquifers. Elements 2(2), 85-90. DOI: 10.2113/gselements.2.2.85

Lu, X., Zang, X., 2005. Environmental geochemistry study of arsenic in Western Hunan mining area, P.R. China. Environ. Geochem. Helth. 27, 313-320. DOI: 10.1007/s10653-004-5735-8

Lumsdone, D.G., Meeussen, J.C.L., Paterson, E., Garden, L.M., Anderson, P., 2001. Use of solid phase characterization and chemical modelling for assessing the behavior of arsenic in contaminated soils. Appl. Geochem. 16, 571-581. DOI: 10.1016/S0883-2927(00)00063-9

Mandal, K.B., Suzuki, K.T., 2002. Arsenic round the world. Talanta 58, 201-235. DOI: 10.1016/S0039-9140(02)00268-0

Marabottini, R., Stazi, S.R., Rapp, R., Grego, S., Moscatelli, M.C., 2013. Mobility and distribution of arsenic in contaminated mine soils and its effects on the microbial pool. Ecotox. Environ. Safe. 96, 147-153. DOI: 10.1016/j.ecoenv.2013.06.016

Martin, M., Violante, A., Ajmone-Marsan, F., Barberis, E., 2014. Surface interactions of arsenite and arsenate on soil colloids. Soil Sci. Soc. Am. J. 78**,** 157-170. DOI:10.2136/sssaj2013.04.0133

Masscheleyn, P.H., Delaune, R.D., Patrick, W.H., 1991. Effect of redox potential and pH on arsenic speciation and solubility in a contaminated soil. Environ. Sci. Technol. 25, 1414-1419. DOI: 10.1021/es00020a008

Mimmo, T., Del Buono, D., Terzano, R., Tomasi, N., Vigani, G., Crecchio, C., Pinton, R., Zocchi, G., Cesco, S., 2014. Rhizospheric organic compounds in the soil-microorganism-plant system: their role in iron availability. Eur. J. Soil Sci. 65, 629-642. DOI: 10.1111/ejss.12158

Morin, G., Calas, G., 2006. Arsenic in soils, mine tailings and former industrial sites. Elements 2(2), 103-107. DOI: 10.2113/gselements.2.2.97

Nazari, A. M., Radzinski, R. Ghahreman, A., in press. Review of arsenic metallurgy: treatment of arsenical minerals and the immobilization of arsenic. Hydrometallurgy DOI: 10.1016/j.hydromet.2016.10.011

Niazi, N.K., Singh, B., Shah, P., 2011. Arsenic speciation ona phytoavailability in contaminated soils using a sequential extraction procedure and XANES spectroscopy. Envirn. Sci, Technol. 45, 7135-7142. DOI: 10.1021/es201677z

Parson, C., Margui Grabulosa, E., Pili, E., Floor, G.H., Roman-Ross, G., Charlet, L., 2013. Quantification of trace arsenic in soils by field-portable X-ray fluorescence spectrometry: considerations for sample preparation and measurement conditions. J. Hazard. Mater. 262, 1213-1222. DOI: 10.1016/j.jhazmat.2012.07.001

Patnurk, D., Dutrizac, J., Gertsman, V., 2008. Syntesys and phase transformations involving scorodite, ferric arsenate and arsenical ferrihydrite: implications for arsenic mobility. Geochim Cosmochim. Acta 72, 2649-2672. DOI:101016/j.gca.2008.03.012

Porfido, C., Allegretta, I., Panzarino, O., Terzano, R., de Lillo, E., Spagnuolo, M., 2016. Bioavailability of arsenic in two Italian industrial contaminated soils, in: Bhattacharya, P., Vahter, M., Jarsjö, J., Kumpiene, J., Ahmad, A., Sparrenbom, C., Jacks, G., Donselaar, M.E., Bundshuh, J., Naidu, R., (Eds.), Arsenic Research and Global Sustainability: Proceedings of the 6th International Congress on Arsenic in the Environment (As2016) CRC Press, London, pp. 342-343.

Radu, T., Diamond, D., 2009. Comparison of soil pollution concentrations determined using AAS and portable XRF techniques. J. Hazard. Mater. 171, 1168-1171. DOI: 10.1016/j.jhazmat.2009.06.062

Savage, K.S., Tingle, T.N., O'Day, P.A., Waychunas, G.A., Bird, D.K., 2000. Arsenic speciation in pyrite and secondary weathering phases, Mother Lode Gold District, Tuolumne County, California. Appl. Geochem. 15, 1219-1244. DOI: 10.1016/S0883-2927(99)00115-8

Savage, K.S., Bird, D.K., O'Day, P.A., 2005. Arsenic speciation in synthetic jarosite. Chem. Geol. 215, 473-498. DOI: 10.1016/j.chemgeo.2004.06.046

Smedley, P.L., Kinninburgh, D.G., 2002. A review of the source, behavior and distribution of arsenic in natural waters. Appl. Geochem.17, 517-568. DOI: 10.1016/S0883-2927(02)00018-5

Solé, V.A., Papillon, E., Cotte, M., Walter, Ph., Susini, J., 2007. A multiplatform code for the analysis of energy-dispersive X-ray fluorescence spectra. Spectochim. Acta B. 62, 63-68. DOI:10.1016/j.sab.2006.12.002

Sparks, D.L., 1996. Mehods of Soil Analysis, Part 3, Chemical Methods. Soil Sciece Society of America, American Society of Agronomy. Madison.

Strawn, D., Doner, H., Zavarin, M., McHugo, S., 2002. Microscale investigation into geochemistry of arsenic, selenium and iron in soil developed in pyritic shale materials. Geoderma 108, 237-257. DOI: 10.1016/S0016-7061(02)00133-7

Terzano, R., Cuccovillo, G., Gattullo, C.E., Medici, L., Tomasi, N., Pinton, R., Mimmo, T., Cesco, S., 2015. Combined effect of organic acids and flavonoids on the mobilization of major and trace elements from soil. Biol. Fert. Soils 51(6), 685-695. DOI:10.1007/s00374-015-1009-0

Vaughan, D.J., 2006. Arsenic. Elements 2(2), 71-75. DOI:10.2113/gselements.2.2.71

Violante, A., Pigna, M., 2002. Competitive sorption of arsenate and phosphate on different clay minerals and soils. Soil Sci. Soc. Am. J. 66(6), 1788-1796

Warshaw, C.M., 1956. The occurrence of jarosite in underclays. Am. Mineral. 41(3-4), 288-296.

Wenzel, W.W., Kirchbaumer, N., Prohaska, T., Stingeder, G., Lombi, E., Adriano, D.C., 2001. Arsenic fractionation in soils using an improved sequential extraction procedure. Anal. Chim. Acta 436, 309-323.

World Health Organization (WHO) 2011. Guidelines for drinking-water quality. WHO, Geneve.

Zobrist, J., Dowdle, P.P., Davis, J.A., Oremland, R.S., 2000. Mobilization of arsenite by dissimilatory reduction of adsorbed arsenate. Environ. Sci. Technol. 34, 4747-4753. DOI: 10.1021/es001068h

Figure caption list

Fig. 1 The mining area of "Crocette" and identification of the sample sites S1, S2, S3 and S4.

Fig. 2 X-ray diffraction patterns of soils and mine tail from "Crocette" gold mine. Letters and symbols refer to illite (I), kaolinite (K), quartz (Q), microcline (M), albite (A), smectite (S), sepiolite (Spl), jarosite (J), Fe-oxides/hydroxides (*).

Fig. 3 As, Fe, S and Si distribution in the four samples acquired with μXRF.

Fig. 4 As vs Fe scatterplot made using K-lines signal (a) which allows to identify three different As/Fe ratios: sites rich in iron (blue group), medium As/Fe ratio (red group) and high As/Fe ratio (green group). The area in which these ratios have been measured are identified (b) using Si map (gray scale) as background (each side of the map measured 1 cm). A magnification of S4 put in evidence a sample portion having a As/Fe ratio of the green group (c).

Fig. 5 Backscattered electron image (a) and chemical maps of As (b), S (c) and Fe (d) of the area characterized by As/Fe ratio of the red group in Figure 4. As and Fe occupied the same sites while As and S are uncorrelated.

Fig. 6 Backscattered electron image of the area where the As/Fe ratio of the green group were identified (a). EDX analysis demonstrates that the bright mineral is scorodite (b).

Table caption list

Table 1 Physical and chemical properties of soils and mine tailing.

Table 2 WDXRF results of major elements and As concentration in the samples.

Table 3 Percentages of total As quantified in each fraction of the Wenzel et al. (2001) sequential extraction procedure (SEP).

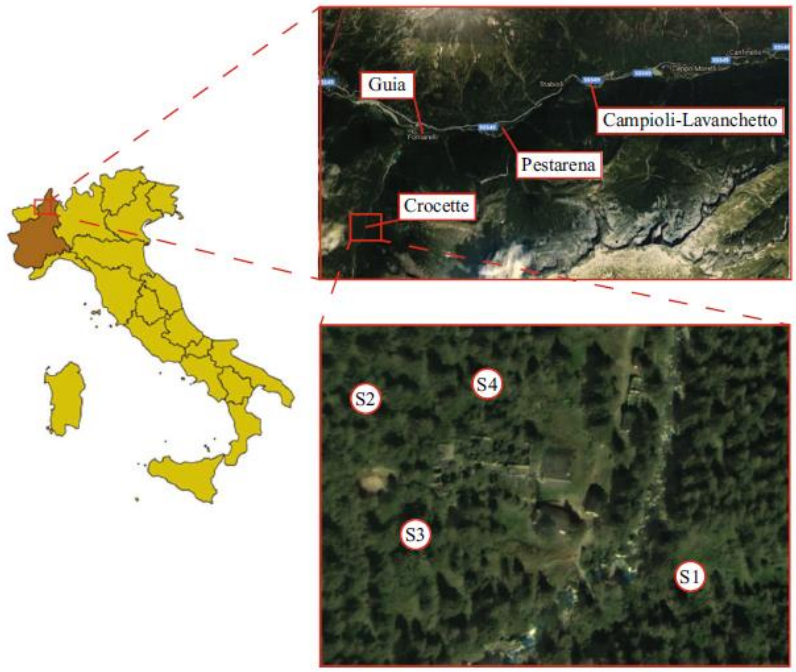
Guia
Campioli-Lavanchetto
Pestarena
Crocette
S2
S4
S3
S1

Fig. 1

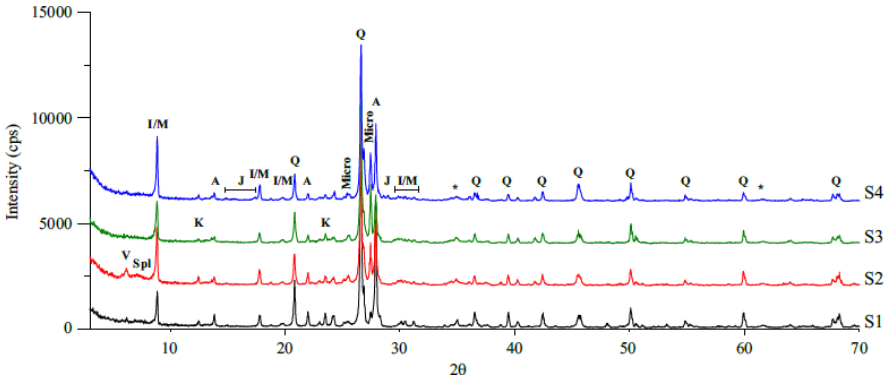
15000
10000
5000
0
Intensity (cps)
10
20
30
40
50
60
70
2θ
I/M
Q
A
J
I/M
I/M
Q
A
Micro
Q
A
Micro
J
I/M
*
Q
Q
Q
Q
Q
Q
Q
*
Q
K
K
V
Spl
S4
S3
S2
S1

Fig. 2

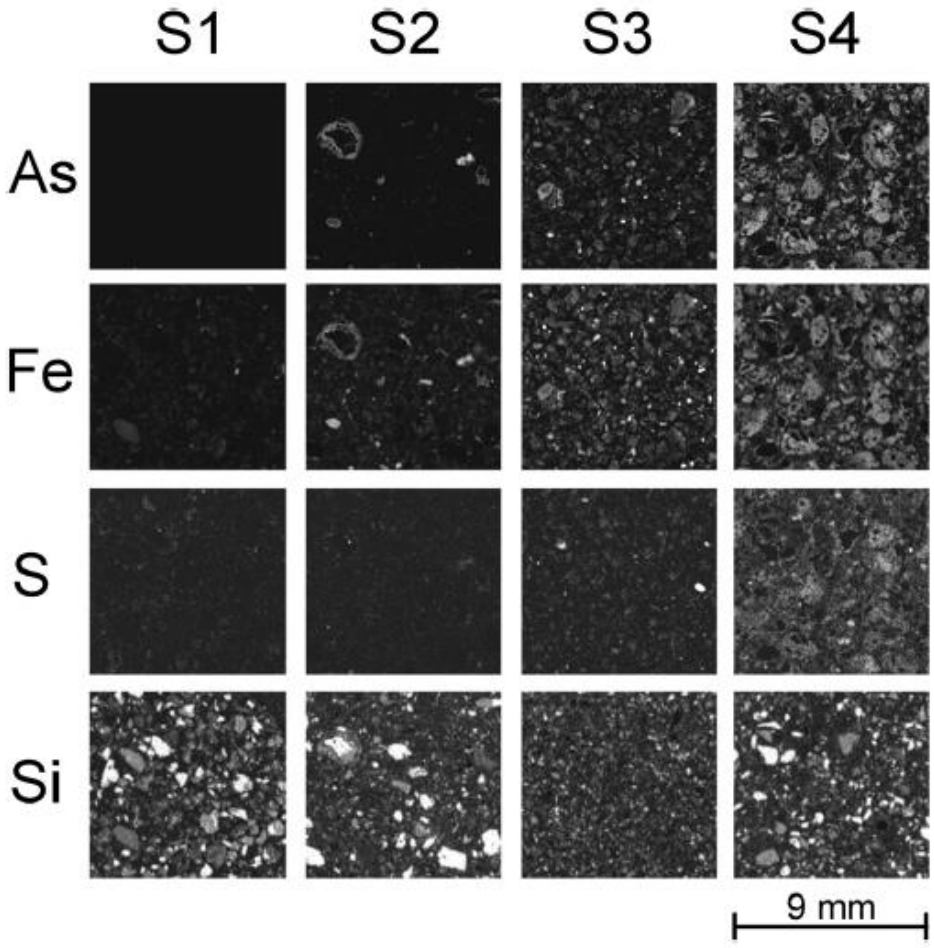

Fig. 3

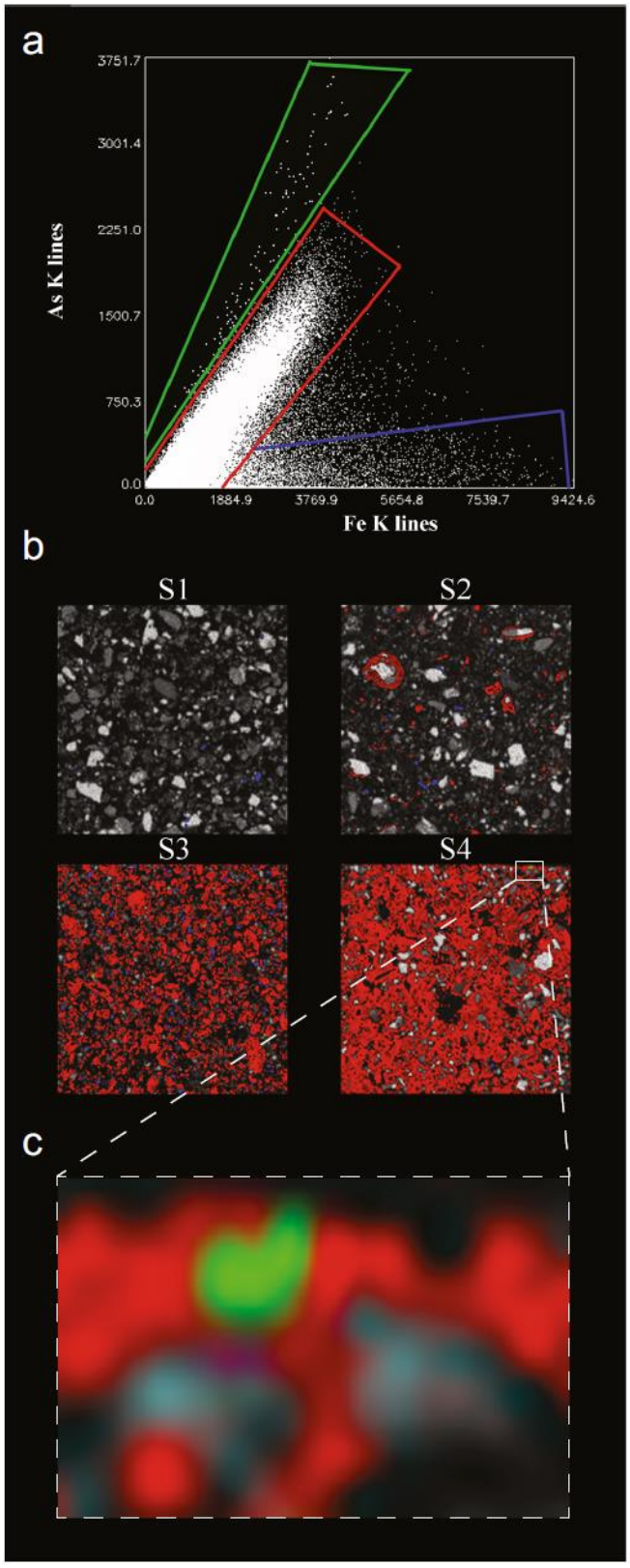
a
3751.7
3001.4
2251.0
1500.7
750.3
0.0
As K lines
0.0
1884.9
3769.9
5654.8
7539.7
9424.6
Fe K lines
b
S1
S2
S3
S4
c

Fig. 4

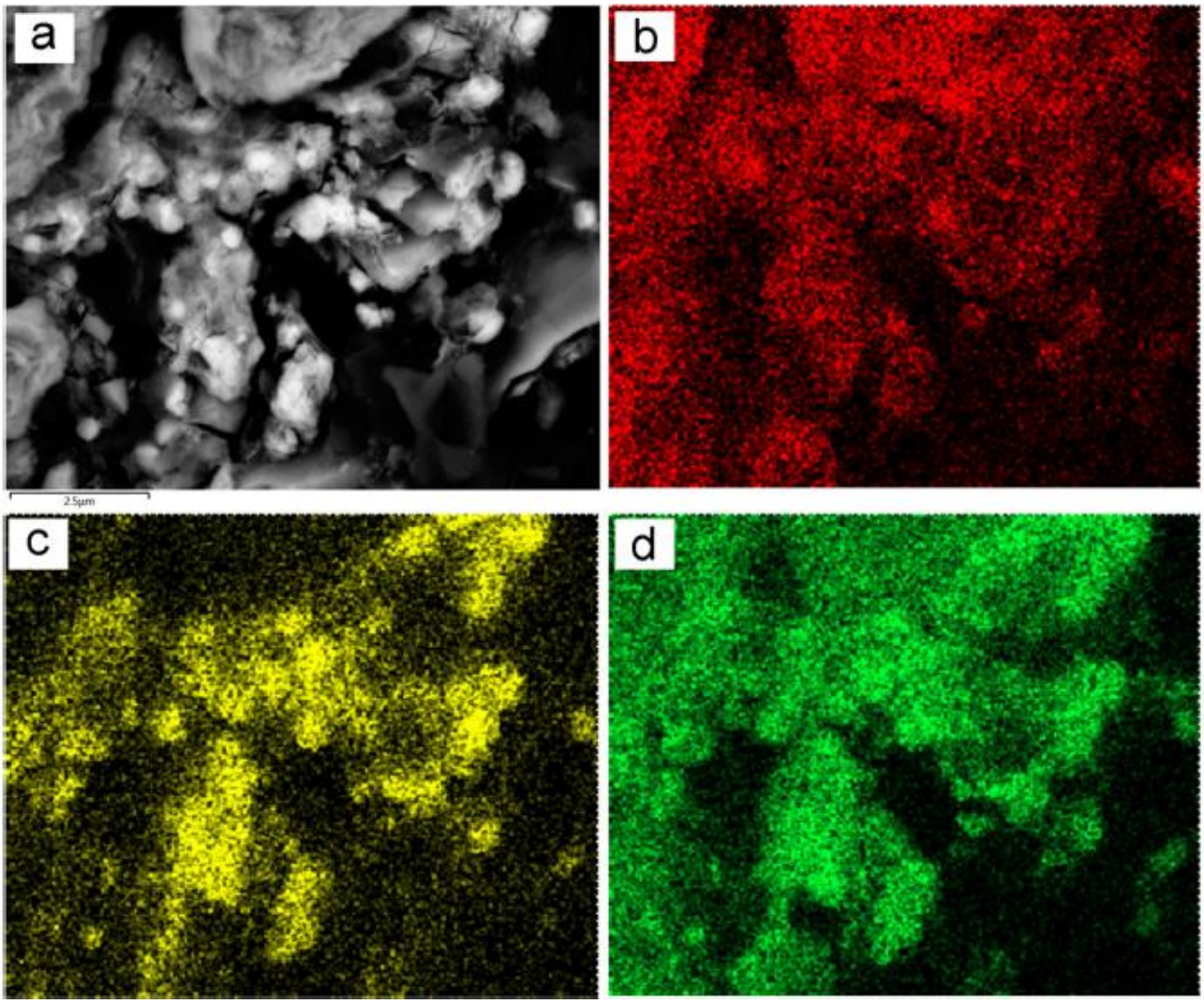

Fig. 5

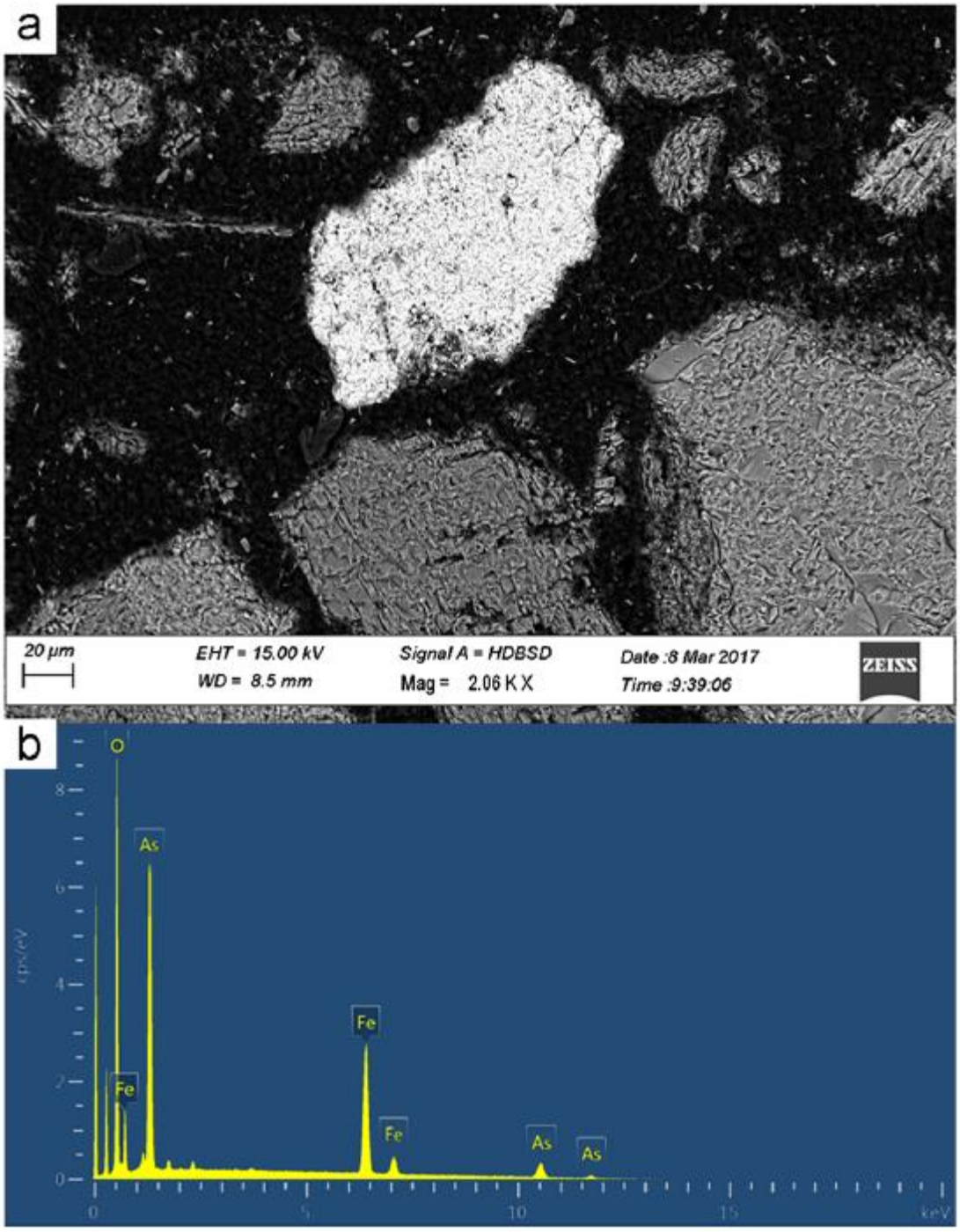
a
20 µm
EHT = 15.00 kV
WD = 8.5 mm
Signal A = HDBSD
Mag = 2.06 K X
Date :8 Mar 2017
Time :9:39:06
ZEISS
b
O
As
Fe
Fe
Fe
As
As
cps/eV
keV

Fig. 6

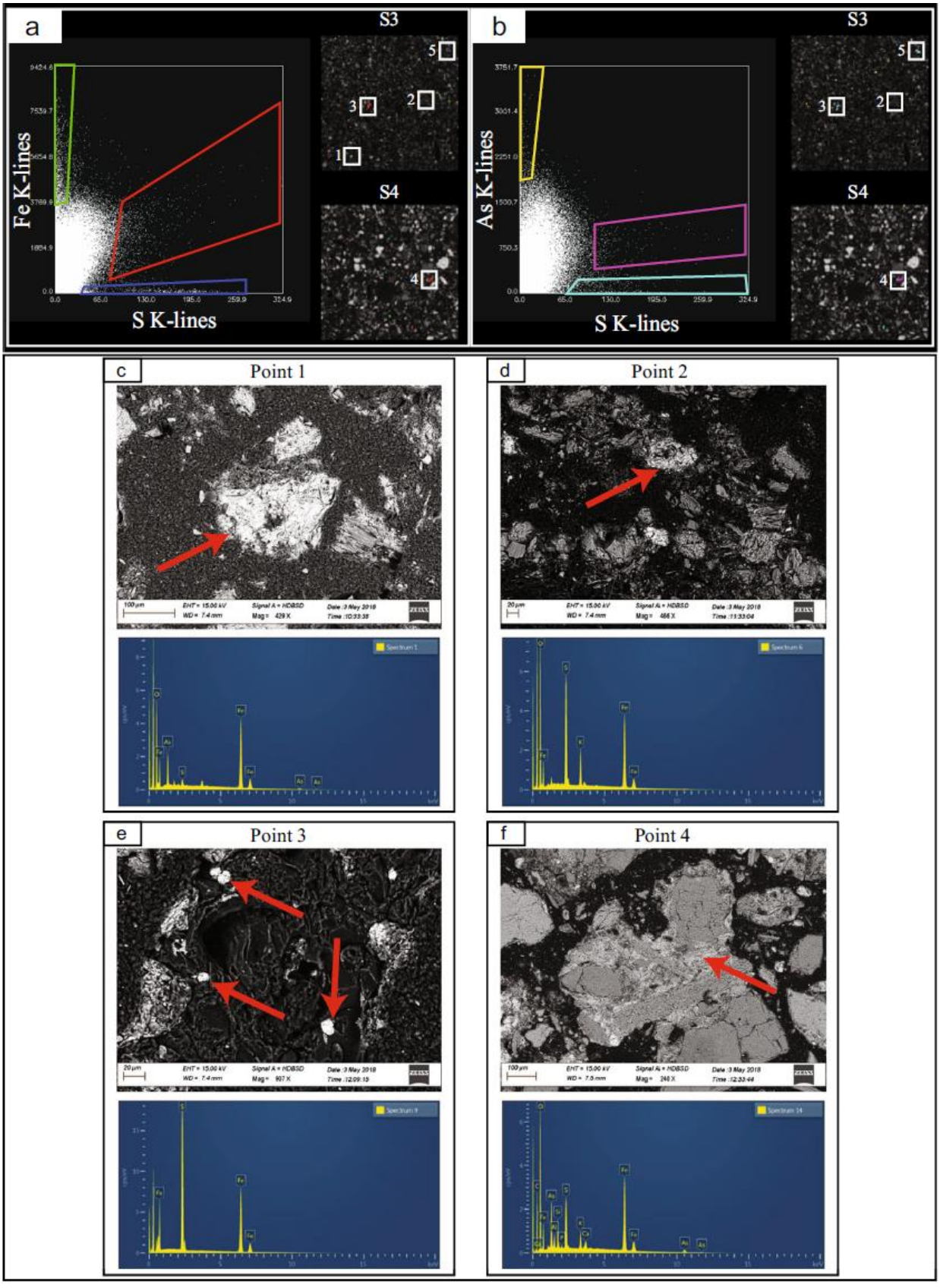
a
S3
5
3
2
1
S4
4
Fe K-lines
S K-lines
b
S3
5
3
2
S4
4
As K-lines
S K-lines
c
Point 1
d
Point 2
e
Point 3
f
Point 4

Fig. 7

Table 1

Table 1 Arsenic and major elements concentration of the soil (S1–S3) and tailing (S4) samples. Some physical and chemical properties are also reported

Sample	As (mg/kg)	SiO_2 (%)	Al_2O_3 (%)	Na_2O (%)	MgO (%)	K_2O (%)	CaO (%)	TiO_2 (%)	Mn_2O (%)	Fe_2O_3 (%)	SO_3 (%)	P_2O_5 (%)	pH (H_2O)	TOC (%)	Sand (%)	Silt (%)	Clay (%)
S1	145	66.17	12.95	4.53	1.09	2.08	0.50	0.45	0.02	3.10	0.26	0.15	4.3	10.9	59.6	25.4	15.0
S2	4640	63.28	13.50	3.36	1.00	4.08	0.59	0.32	0.04	3.86	0.26	0.15	3.7	5.4	59.9	28.3	11.9
S3	13,300	52.23	12.16	1.93	0.52	5.12	0.50	0.35	0.03	6.37	0.65	0.26	4.3	4.7	65.7	24.9	9.4
S4	40,200	53.62	9.51	2.23	0.29	3.69	0.41	0.31	0.02	9.61	1.59	0.22	3.6	2.5	56.0	33.3	10.7

Table 2

Extraction step	Description	S1 % of total As	S2	S3	S4
1	Non-specifically sorbed	2.2 ± 0.2	0.6 ± 0.2	0.2 ± 0.1	0.3 ± 0.1
2	Specifically sorbed	10.7 ± 2.1	25.2 ± 2.7	11.9 ± 2.3	7.6 ± 3.9
3	Associated to amorphous Fe oxides/hydroxides	49.8 ± 0.8	67.2 ± 2.9	85.5 ± 1.5	87.1 ± 4.8
4	Associated to well crystalline Fe oxides/hydroxides	27.9 ± 1.1	1.6 ± 0.3	1.4 ± 0.8	4.7 ± 1.2
5	Residual	9.4 ± 1.2	5.4 ± 1.1	1.0 ± 0.6	0.3 ± 0.2